Available online at www.sciencedirect.com
SCIENCE DIRECT®
Thin Solid Films 429 (2003) 273–281
thin solid films
www.elsevier.com/locate/tsf

Very thin solid-on-liquid structures: the interplay of flexural rigidity, membrane force, and interfacial force

R. Huang[a,*], Z. Suo[b]

[a]*Aerospace Engineering and Engineering Mechanics Department, The University of Texas, Austin, TX 78712, USA*
[b]*Mechanical and Aerospace Engineering Department and Princeton Materials Institute, Princeton University, Princeton, NJ 08544, USA*

Received 6 December 2002; received in revised form 16 January 2003; accepted 20 January 2003

Abstract

This paper studies a solid film lying on a liquid layer, which in turn lies on a solid substrate. It is well known that, subject to a compressive membrane force, the solid film wrinkles, dragging the liquid underneath to flow. When the solid film is very thin, the ratio between the number of atoms at the surface and that in the bulk becomes significant, so that surface stress contributes to the membrane force. When the liquid layer is very thin, the two interfaces bounding the liquid interact with each other through forces of various physical origins. We formulate the free energy of the system, and carry out a linear perturbation analysis. A dimensionless parameter is identified to quantify the relative importance of flexural rigidity, membrane force, and interfacial force on stability of the structure. Depending on the nature of the interfacial force, several intriguing behaviors are possible; for example, the solid film may remain flat under a compressive membrane force, or form wrinkles under a tensile membrane force. We estimate the dimensionless parameter for interfacial forces of several specific origins, including photon dispersion, electrical double layer, and electron confinement. Emphasis is placed on identifying the thickness ranges of the solid film and of the liquid layer within which these forces are important.

Keywords: Surface stress; Interfacial force; Stability; Nanostructures

1. Introduction

In studying nanostructures, one often encounters interactions that are different from those acting in macrostructures (e.g. gravity) and those acting in atomic structures (e.g. chemical bonds). Reflecting upon centuries of investigations of the role of gravity in the motion of celestial bodies, one can readily see that elucidating the roles of interactions of diverse origins in nanostructures will be a main challenge for some time [1]. The best-studied example so far involves photon dispersion and electrical double layers in stabilizing colloids [2–4]. A recent example involves surface stresses in stabilizing nanoscale domains on solid surfaces [5,6].

This paper explores another class of structures, i.e. solid-on-liquid (SOL) structures. Fig. 1a illustrates a SOL structure. The structure can be fabricated by wafer bonding or by deposition. One example of such structures, a strained SiGe film on a layer of borophosphorosilicate glass, has been studied for optoelectronic applications [7,8], in which the glass flows at elevated temperatures. A more common example of such structures is a metallic film covered by a layer of native oxide, where the metal creeps at elevated temperatures. One common observation is that, subject to a compressive membrane force, the solid film wrinkles, dragging the liquid underneath to flow, while the solid and the liquid remain in contact (Fig. 1b).

Recall that a thin liquid layer, lying on a solid substrate by itself, can rupture to form islands and dry spots [9–12]. The instability is driven by long-range attractive interactions between the two interfaces that bound the liquid layer. The surface energy of the liquid can stabilize perturbations of short wavelengths, but not those of long wavelengths. As a result, perturbations of long wavelengths grow and the liquid layer is unstable.

*Corresponding author. Tel.: +1-512-471-7558; fax: +1-512-471-5500.
E-mail address: ruihuang@mail.utexas.edu (R. Huang).

0040-6090/03/$ - see front matter © 2003 Elsevier Science B.V. All rights reserved.
doi:10.1016/S0040-6090(03)00065-8

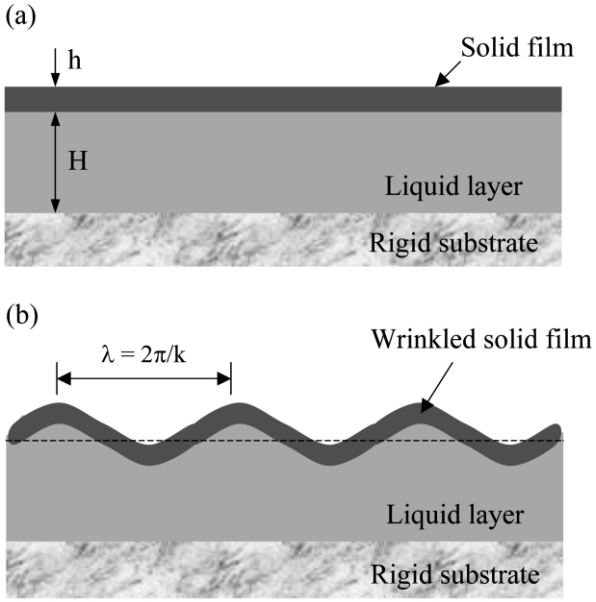

Fig. 1. Illustration of a solid-on-liquid thin film structure: (a) flat and reference state; (b) wrinkled state.

If the liquid layer is covered by a thin solid film, several differences are expected. The flexural rigidity of the solid film provides resistance against perturbations of short wavelengths. If the solid film is subject to a residual stress, tension stabilizes and compression destabilizes the film with perturbations of intermediate wavelengths. The long-range interactions between the interfaces can be attractive or repulsive, destabilizing or stabilizing the film with perturbations of long wavelengths. Yet another difference is about surface energy. The air–liquid interface is now replaced by the solid–liquid interface plus the solid–air interface. As first pointed out by Gibbs [13], the way the energy changes at a solid–liquid interface differs from that at an air–liquid interface. At an air–liquid interface, the energy increases when some liquid molecules inside the bulk emerge to the interface and increase the area. Thus, the change of the surface energy at an air–liquid interface is the surface energy density times the area change, where the surface energy density is a constant. For a solid–liquid interface, however, the number of atomic sites is fixed. The area of the interface is changed by stretching or compressing the inter-atomic distance, which leads to elastic strain at the interface. Consequently, it is the elastic strain and the surface stress that are relevant for the solid–liquid interface [14–18]. In principle, this conservation of atomic sites prevails even for a monolayer solid film on a liquid layer, so long as the solid film remains intact. Unlike the surface energy density at an air-liquid interface, which is always positive and tends to stabilize the liquid layer, the surface stress at a solid–liquid interface can be either positive or negative [19–21], and thus can either stabilize or destabilize the solid film and the liquid layer. Therefore, even a monolayer solid film on a liquid layer can qualitatively change the stability behavior of the liquid layer.

Recently, we and others have studied the stability of a SOL structure by considering the elastic deformation of the solid and the viscous flow of the liquid, but ignoring the effects of surface stresses and interfacial forces [22–25]. The analysis is valid as long as both the solid film and the liquid layer are sufficiently thick. In that case, a compressed solid film is always unstable and forms wrinkles. A critical wavelength is determined by the competition between the decreasing strain energy of compression and the increasing strain energy of bending in the solid film. The liquid layer only affects the time scale of wrinkling.

This paper aims to ascertain how thin the solid film has to be for the surface stresses to be important, and how thin the liquid layer has to be for the interfacial forces to be important. Section 2 formulates the free energy of the system, including the bulk elastic energy, the surface energy, and the interaction energy. Section 3 performs a linear perturbation analysis and discusses the relative importance of the various energetic forces. Section 4 considers interfacial forces of several specific origins and estimates their importance.

2. Free energy of SOL structures

Refer to Fig. 1 again. A thin solid film of thickness h lies on a liquid layer of thickness H, which in turn lies on a planar substrate. To focus on more novel aspects of the system, we neglect the elasticity in both the liquid and the substrate, i.e. the liquid is viscous and the substrate is rigid. Take the configuration with all interfaces flat and parallel as the reference state (Fig. 1a). At the wrinkled state (Fig. 1b), the solid film deflects, and the free energy in the system changes. The energy change consists of the changes in the bulk elastic energy within the solid film (U_B), the surface energy at the solid–liquid interface and the solid–air interface (U_S), and the interaction energy associated with interfacial forces (U_L), i.e.

$$\Delta U = \Delta U_B + \Delta U_S + \Delta U_L \tag{1}$$

If the total free energy increases for any arbitrary wrinkle, the flat film is stable, and the wrinkle will decay. Otherwise, the flat film is unstable, and the wrinkle will grow. Next we discuss the free energy term by term.

First consider the elastic energy stored in the bulk of the solid film. Assume that the solid film is isotropic and elastic with Young's modulus E and Poisson's ratio ν. Let x and y be the coordinates in the middle plane of

the film and z the coordinate perpendicular to the middle plane. The film at the reference state (Fig. 1a) is under an inplane strain, $\varepsilon_{\alpha\beta}$, where α and β stand for x or y. As the wrinkled state (Fig. 1b), the solid film has a deflection, $w(x,y)$, in the z direction. Meanwhile, the film may have some inplane displacements, $u_x(x,y)$ and $u_y(x,y)$. Using the von Karman plate theory [26], from the reference state to the wrinkled state the strain in the film changes by

$$\Delta\varepsilon_{\alpha\beta}=\frac{1}{2}\left(\frac{\partial u_\alpha}{\partial x_\beta}+\frac{\partial u_\beta}{\partial x_\alpha}+\frac{\partial w}{\partial x_\alpha}\frac{\partial w}{\partial x_\beta}\right)-\frac{\partial^2 w}{\partial x_\alpha \partial x_\beta}z, \tag{2}$$

where $z=0$ at the middle plane and $z=\pm h/2$ at the top and bottom surfaces of the solid film. The bulk elastic energy of the solid film consists of the inplane strain energy and the bending energy. From the reference state to the wrinkled state, the change of the bulk elastic energy per unit area is

$$\Delta U_B=\frac{\sigma_{\alpha\beta}h}{2}\left(\frac{\partial u_\alpha}{\partial x_\beta}+\frac{\partial u_\beta}{\partial x_\alpha}+\frac{\partial w}{\partial x_\alpha}\frac{\partial w}{\partial x_\beta}\right)+\frac{D}{2}\times\left[\frac{\partial^2 w}{\partial x^2}+\frac{\partial^2 w}{\partial y^2}\right]^2+2(1-\nu)\left[\left(\frac{\partial^2 w}{\partial x\partial y}\right)^2-\frac{\partial^2 w}{\partial x^2}\frac{\partial^2 w}{\partial y^2}\right] \tag{3}$$

where $\sigma_{\alpha\beta}$ is the inplane residual stress in the film at the reference state, and $D=\dfrac{Eh^3}{12(1-\nu^2)}$ is the flexural rigidity. We adopt the convention that a repeated Greek subscript implies summation over the two in-plane dimensions.

Following Cahn [14], we define the surface energy density referring to the surface area of the undeformed state. The surface energy density is a function of surface strain. Expanding the surface energy density in terms of the surface strain, and keeping only the linear term, we have

$$U_s=\Gamma_0+f_{\alpha\beta}\varepsilon^s_{\alpha\beta}, \tag{4}$$

where Γ_0 is the surface energy density at the undeformed state, $f_{\alpha\beta}$ is the surface stress, and $\varepsilon^s_{\alpha\beta}$ is the strain at the solid surface.

In the present SOL structure, as the film wrinkles, the strain changes at both top and bottom surfaces of the solid film, and the amount of the change is obtained from Eq. (2) by setting $z=\pm h/2$. Combining the changes at the two solid surfaces, the total change of the surface energy per unit area is

$$\Delta U_s=\frac{1}{2}\left(\frac{\partial u_\alpha}{\partial x_\beta}+\frac{\partial u_\beta}{\partial x_\alpha}+\frac{\partial w}{\partial x_\alpha}\frac{\partial w}{\partial x_\beta}\right)\bar{f}_{\alpha\beta}-\frac{\partial^2 w}{\partial x_\alpha \partial x_\beta}\frac{h}{2}\tilde{f}_{\alpha\beta} \tag{5}$$

where $\tilde{f}_{\alpha\beta}$ equals the surface stress of the top surface (solid–air interface) minus that of the bottom surface (solid–liquid interface), and is the $\bar{f}_{\alpha\beta}$ sum of the two surface stresses. The first term in Eq. (5) corresponds to inplane deformation, and the second term corresponds to bending. Thus, the experimental measurements of surface stresses based on bending of a cantilever beam or plate [21] are actually measuring $\tilde{f}_{\alpha\beta}$, i.e. the difference between the surface stresses at the top and bottom surfaces of the beam or plate.

The long-range forces between the interfaces separated by a liquid lead to the interaction energy. Following the common practice in the literature [2–4], we take the interaction energy per unit area as a function of the separation, $U_L(H)$. Thus, from the reference state to the wrinkled state of the SOL structure, the change of the interaction energy per unit area is

$$\Delta U_L=U_L(H+w)-U_L(H). \tag{6}$$

The explicit expression of the interaction energy will be given later for specific interfacial forces.

3. Linear perturbation analysis

An arbitrary deflection field, $w(x,y)$, can be represented by the summation of the Fourier components of different modes along different directions. For linear perturbation analysis, we study the behavior of a single component, i.e. a sinusoidal perturbation of a constant wavelength. Since the SOL structure is isotropic in the x–y plane, any direction of the sinusoidal wave is equivalent, and we choose the direction to coincide with the x-direction. Meanwhile, an inplane displacement of the same wavelength is required by kinetics. Following Huang and Suo [25], we write

$$w=q_1\sin(kx), \tag{7}$$

$$u=q_2\cos(kx), \tag{8}$$

where q_1 and q_2 are the amplitudes of the perturbation, and k is the wavenumber. Compute the free energy change associated with the perturbation by integrating the energy density over one period of the perturbation, and then divide by the period. To the leading order in the perturbation amplitudes, the free energy change per unit area is given by

$$\Delta\bar{U}=\frac{q_1^2}{4}[Dk^4+Nk^2+U_L''], \tag{9}$$

where $N=\sigma h+\bar{f}$ is the resultant membrane force of the solid film, $\sigma=\sigma_{xx}$ is the residual stress in the solid film

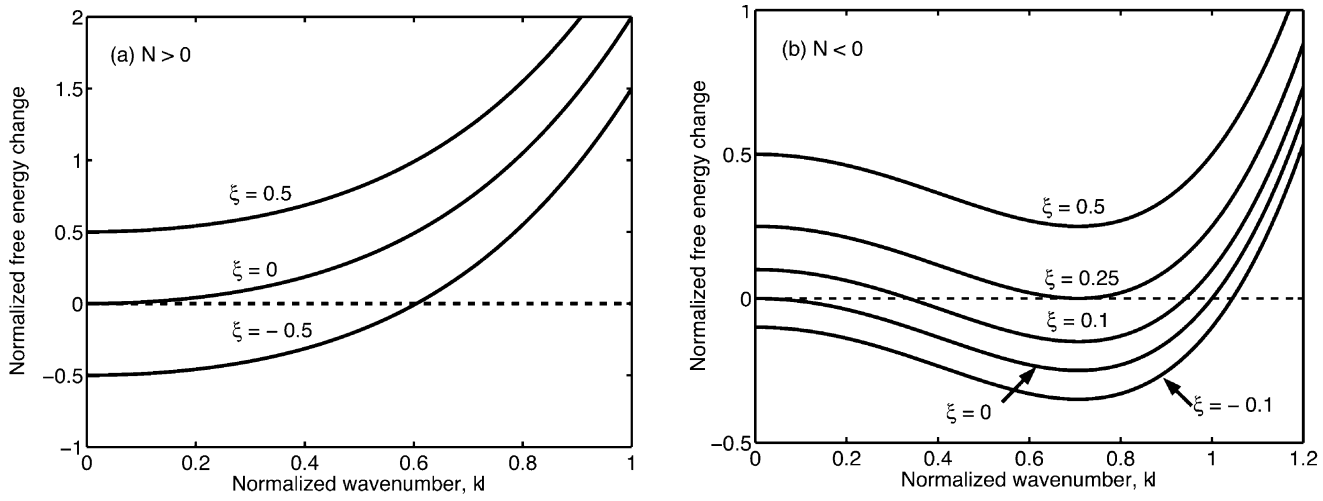

Fig. 2. Normalized free energy change vs. normalized wavenumber for various values of ξ: (a) $N>0$ and (b) $N<0$.

at the reference state, $\bar{f}=\bar{f}_{xx}$ is the sum of the surface stresses at the top and bottom surfaces of the solid film, and $U_L''=\partial^2 U_L/\partial H^2$. Note that, due to the periodicity of the perturbation, the amplitude of the inplane displacement, q_2, disappears after integration, and so does $\tilde{f}_{xx}$ in the second term of Eq. (5). Thus, the effect of the surface stress only depends on its contribution to the resultant membrane force and will be important if $\bar{f}$ is comparable with σh. For representative values, $\bar{f}=1$ N/m and $\sigma=100$ MPa, the thickness of the solid film has to be approximately 10 nm or less for the surface stress to be important.

We note that, from Eq. (9), the flexural rigidity of the solid film, D, stabilizes the film against perturbations of large wavenumbers. Depending on its sign, the resultant membrane force, N, either stabilizes or destabilizes the flat film with perturbations of intermediate wavenumbers. Depending on the sign of U_L'', the long-range interaction either stabilizes or destabilizes the flat film with perturbations of small wavenumbers.

A comparison between the first two terms in the bracket of Eq. (9) defines a length, namely,

$$l=\left(\frac{D}{|N|}\right)^{1/2}. \tag{10}$$

Neglecting the effect of interaction energy, when $N<0$, the film is stable against large wavenumber perturbations, but unstable for small wavenumber perturbations, and the critical wavenumber is $k_c l=1$. The critical wave number is the same as that given by the Euler instability as a result of the competition between bending and in-plane strain energy, except for the contribution of the surface stress in the membrane force.

A comparison between the first and the third terms in the bracket of Eq. (9) defines another length, namely,

$$b=\left(\frac{D}{|U''_L|}\right)^{1/4}, \tag{11}$$

When $N=0$ and $U_L''<0$, the competition between bending and interaction energy sets another critical wavenumber: $k_c b=1$. Small wavenumber perturbations grow and large wavenumber perturbations decay.

When considering all three terms in Eq. (9), we define a dimensionless parameter,

$$\xi=\frac{DU_L''}{N^2}. \tag{12}$$

One can confirm that the magnitude of ξ is $(l/b)^4$, and the sign of ξ is the same as that of U_L''. When U_L is concave up, $U_L''>0$ and $\xi>0$. When U_L is concave down, $U_L''<0$ and $\xi<0$.

The free energy change in Eq. (9) is quadratic in terms of k^2. In terms of l and ξ, Eq. (9) can be expressed as

$$\Delta\bar{U}=\frac{q_1^2 D}{4l^4}\left[(kl)^4+\mathrm{Sign}(N)(kl)^2+\xi\right]. \tag{13}$$

Fig. 2 shows the free energy change as a function of the wavenumber for various values of ξ. We distinguish five cases as follows.

3.1. Case 1: $N>0$ and $\xi>0$

When the net membrane force is tensile and the interaction energy is concave up, they both stabilize the flat film. The film is stable against perturbations of all wavenumbers. Fig. 2a shows that, in this case, $\Delta\bar{U}>0$ for all wavenumbers.

3.2. Case 2: $N>0$ and $\xi<0$

In this case, the interaction energy is concave down and tends to destabilize the film with perturbations of all wavenumbers. While the flexural rigidity of the solid film stabilizes the film against perturbations of large wavenumbers and the tensile membrane force stabilizes against perturbations of intermediate wavenumbers, the film is unstable with perturbations of small wavenumbers. Consequently, even when the resultant membrane force is tensile, the film may still wrinkle if the long-range interaction energy is concave down. As shown in Fig. 2a, when $\xi<0$, the curve intersects with the line $\Delta\bar{U}=0$at one point, which is the critical wave number and is given by

$$(kl)^2=\frac{1}{2}\left(\sqrt{1-4\xi}-1\right). \tag{14}$$

3.3. Case 3: $N<0$ and $\xi>0.25$

The membrane force is compressive and tends to destabilize the film with perturbations of intermediate wavenumbers. However, the flexural rigidity of the solid stabilizes the film against perturbations of large wavenumbers, and the concave-up interaction energy stabilizes against perturbations of small wavenumbers. Provided that the combined effect of the flexural rigidity and the interaction energy prevails over the effect of the compressive membrane force, the flat film is stable against perturbations of all wavenumbers. As shown in Fig. 2b, when $\xi>0.25$, $\Delta\bar{U}>0$ for all wavenumbers.

3.4. Case 4: $N<0$ and $0.25>\xi>0$

In this case, the combined stabilizing effect of the flexural rigidity and the concave-up interaction energy cannot cover perturbations of all wavenumbers, and the compressive membrane force destabilizes the film with perturbations of some intermediate wavenumbers. As shown in Fig. 2b, when $0.25>\xi>0$, the curve intersects with the line $\Delta\bar{U}=0$ at two wavenumbers:

$$(kl)^2_{1,2}=\frac{1}{2}\left(1\pm\sqrt{1-4\xi}\right). \tag{15}$$

The free energy decreases as perturbations of intermediate wavenumbers ($k_1<k<k_2$) grow.

3.5. Case 5: $N<0$ and $\xi<0$

When the resultant membrane force is compressive and the interaction energy is concave down, they both destabilize the flat film. While the flexural rigidity stabilizes the film against perturbations of large wavenumbers, the film is unstable with perturbations of small wavenumbers. As shown in Fig. 2b, when $\xi<0$, the curve intersects with the line $\Delta\bar{U}=0$ at only one wavenumber given by

$$(kl)^2=\frac{1}{2}\left(\sqrt{1-4\xi}+1\right). \tag{16}$$

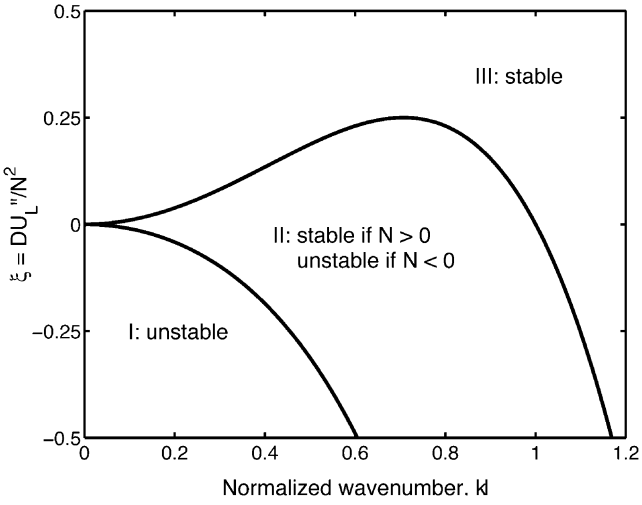

Fig. 3. Stable and unstable regions in the ξ-kl diagram.

To summarize, Fig. 3 shows the stable and unstable regions in the $\xi-kl$ diagram. In region I, the film is unstable. In region III, the film is stable. In region II, the film is unstable if $N<0$ and stable if $N>0$.

4. Specific interfacial forces and representative values of ξ

From the linear perturbation analysis in the previous section, the stability of the very thin SOL structures is mainly determined by the value of ξ. In this section we discuss several specific interfacial forces and give representative values of ξ.

4.1. Photon dispersion

The change of the number of photons in the electromagnetic oscillation modes in a structure made of several media leads to a configurational force, known as the dispersion force or the van der Waals force [27]. For example, for two semi-infinite plates at separation H, the interaction energy per unit area is

$$U_L(H)=-\frac{A}{12\pi H^2} \tag{17}$$

where A is the Hamaker constant, which depends on the

dielectric spectra of the media [4,28]. When two identical media interact across a film of another medium the dispersion force is attractive ($A>0$). When two dissimilar media interact across a film of a third medium the dispersion force can be either attractive or repulsive ($A<0$). In the following discussions, we consider the attractive dispersion force only.

The system under consideration consists of four media: the substrate, the liquid layer, the solid film, and the air. Although the interaction energy of such structures can be developed, here we are mainly interested in estimating the order of magnitude and will use Eq. (17) as an approximation. Substituting Eq. (17) into Eq. (12), we obtain that, for the dispersion force,

$$\xi = -\frac{Eh^3A}{24\pi(1-\nu^2)\left(\sigma h+\bar{f}\right)^2H^4}. \tag{18}$$

For attractive dispersion forces, $A>0$ and $\xi<0$. Consequently, there exists a critical wavenumber, k_c. The flat film is stable against perturbations of larger wavenumbers ($k>k_c$), but unstable with perturbations of smaller wavenumbers ($k<k_c$). When the resultant membrane force is tensile, the critical wavenumber is given by Eq. (14). When the resultant membrane force is compressive, the critical wavenumber is given by Eq. (16). When the resultant membrane force is zero, the critical wavenumber is given by $k_cb=1$, where b is a length defined in Eq. (11).

Using representative values, $A=10^{-20}$ J, $E=100$ GPa, $\sigma=\pm100$ MPa, $h=10$ nm, $H=10$ nm, and $\nu=0.3$, and neglecting the surface stress ($\bar{f}=0$), we have $l\approx95$ nm, $b\approx490$ nm, and $\xi=-(l/b)^4\approx-1.5\times10^{-3}$. With a tensile membrane force ($\sigma=100$ MPa), from Eq. (14), the critical wavelength ($\lambda_c=2\pi/k_c$) is approximately 15 μm. With a compressive membrane force ($\sigma=-100$ MPa), from Eq. (16), the critical wavelength is approximately 0.6 μm. Without any membrane force ($N=0$), the critical wavelength is approximately 3.1 μm. Therefore, when the membrane force is tensile, although the flat film may still wrinkle under the attractive dispersion force, the wavelength of the wrinkle is very long compared to the wrinkle under compressive membrane force, i.e. the film is relatively flat.

As shown in Fig. 2, the normalized critical wavenumber, k_cl, increases as the magnitude of ξ increases. From Eq. (18), the magnitude of ξ is proportional to the Hamaker constant A and inversely proportional to H^4. Therefore, the critical wavenumber is much more sensitive to H than it is to A. When the liquid layer is thick, ξ is small and the effect of the interaction energy is negligible. When the thickness of the liquid layer is less than 10 nm, the magnitude of ξ increases dramatically, and the effect of the interaction energy becomes important.

4.2. Electrical double layer

When a body is immersed in a polar solvent such as water, the interface often acquires a charge, by either adsorbing or desorbing ions according to chemical equilibrium with the surrounding solution. Ions of opposite charge dissolved in solvent, known as counter-ions, are attracted toward the interface, forming a diffuse layer of charge adjacent to the interface. The surface charge and the diffuse layer of counter-ions constitute an electrical double layer. The thickness of the double layer depends on the concentration of ions in solution: more ions available give a thinner double layer. When two such interfaces approach each other, they repel. The complete expression for the repulsive force is complicated and is best solved numerically [29]. An approximate expression for the interaction energy, which is valid for symmetric z:z electrolytes (e.g. NaCl) and large separations ($H>\kappa^{-1}$), is given by [2,4]

$$U_L(H)=B\exp(-\kappa H) \tag{19}$$

and

$$B=64\kappa^{-1}nk_BT\left[\tanh\left(\frac{ze\phi_s}{4k_BT}\right)\right]^2, \tag{20}$$

$$\kappa^{-1}=\sqrt{\frac{\varepsilon k_BT}{2nz^2e^2}}, \tag{21}$$

where n is the number density and z is the valence of the cationic species, ε is the dielectric permittivity of the solvent, ϕ_s is the surface potential, e is the electronic charge, k_B is Boltzmann's constant, and T is the temperature. The thickness of the double layer is measured by the Debye length, κ^{-1}.

Assuming that, in a SOL structure, the two interfaces bounding the liquid layer interact with each other through electrical double layers, and using Eq. (19) as the interaction energy, we obtain that

$$\xi=\xi_0\exp(-\kappa H), \tag{22}$$

where

$$\xi_0=\frac{Eh^3B\kappa^2}{12(1-\nu^2)\left(\sigma h-\bar{f}\right)^2}. \tag{23}$$

In this case, ξ is always positive, decreasing exponentially as H increases.

When the resultant membrane force is tensile ($N>0$), as shown in Fig. 2a, positive ξ leads to positive free energy change for all wavenumbers. Thus, the flat film is stable against perturbations of all wave numbers, regardless of the thickness H.

When the resultant membrane force is compressive ($N<0$), as shown in Fig. 2b, the flat film is stable against perturbations of all wavenumbers if $\xi>0.25$, but is unstable with perturbations of intermediate wavenumbers if $0.25>\xi>0$. Therefore, when $\xi_0>0.25$, there exists a critical thickness for the liquid layer, $H_c=\kappa^{-1}\ln(4\xi_0)$. When $H<H_c$, $\xi>0.25$ and the flat film is stable. When $H>H_c$, $0.25>\xi>0$ and the flat film is unstable. When $\xi_0<0.25$, however, $0<\xi<0.25$ for any thickness H, and the flat film is unstable.

Using representative values, $h=10$ nm, $\sigma=-100$ MPa, $\varepsilon=10^{-9}$ C^2/Nm^2, $\phi_s=0.1$ V, $E=100$ GPa, $\nu=0.3$, and $T=300$ K, we have $\kappa^{-1}=3.665$ nm and $\xi_0=2.224$ for a 1:1 electrolyte ($z=1$) of concentration 0.01 M ($n=6.02\times10^{24}$ m^{-3}). The critical thickness is $H_c=8$ nm. At a lower electrolyte concentration, $n=6.02\times10^{23}$ m^{-3}, we have $\kappa^{-1}=11.59$ nm and $\xi_0=0.07$, i.e. the double layer force becomes weaker but longer ranged.

4.3. Combination of photon dispersion and electrical double layer

The well-known DLVO theory of colloidal stability is based on the assumption that the net force between particles immersed in a polar liquid is given by the algebraic sum of the repulsive double layer force and the attractive dispersion force [3,30]. Using the representative values of the parameters as before, Fig. 4a shows the combined interaction energy (U_L) from Eqs. (17) and (19) as a function of separation H, and Fig. 4b shows its curvature (U_L''). The combined interaction energy is concave down for thin liquid layers, but concave up for thick liquid layers. In Fig. 4, the critical thickness, H_c, is approximately 2 nm.

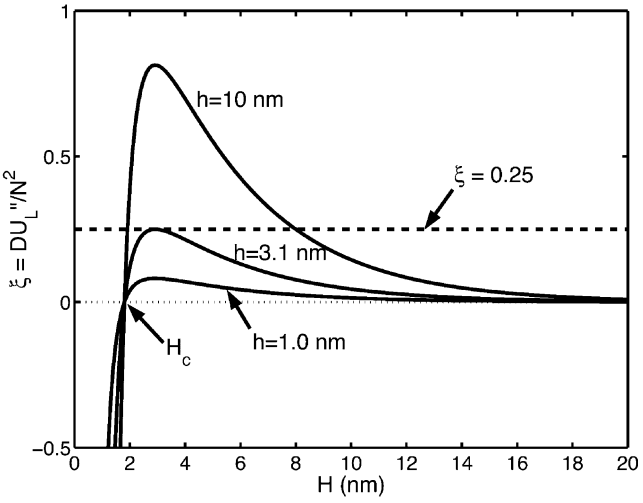

Fig. 5. Dimensionless parameter ξ as a function of H for various values of h, under the combined interaction of photon dispersion and electrical double layer.

Fig. 5 shows the ξ–H curves for various values of h, using the same parameters in Fig. 4 and $E=100$ GPa, $\nu=0.3$, $\sigma=\pm100$ MPa, $\bar{f}=0$. When the membrane force is tensile, the flat film is stable against perturbations of all wavenumbers if $H>H_c$, but unstable if $H<H_c$. The value of the critical thickness H_c is independent of h. When the membrane force is compressive, there exists a critical thickness of the solid film, h_c. For example, in Fig. 5, $h_c=3.1$ nm. When $h>h_c$, the maximum value of ξ is greater than 0.25, and there exists a thickness window for H, within which $\xi>0.25$ and the flat film is stable against perturbations of all wavenumbers. When $h<h_c$, however, $\xi<0.25$ for any H, and the flat film is unstable.

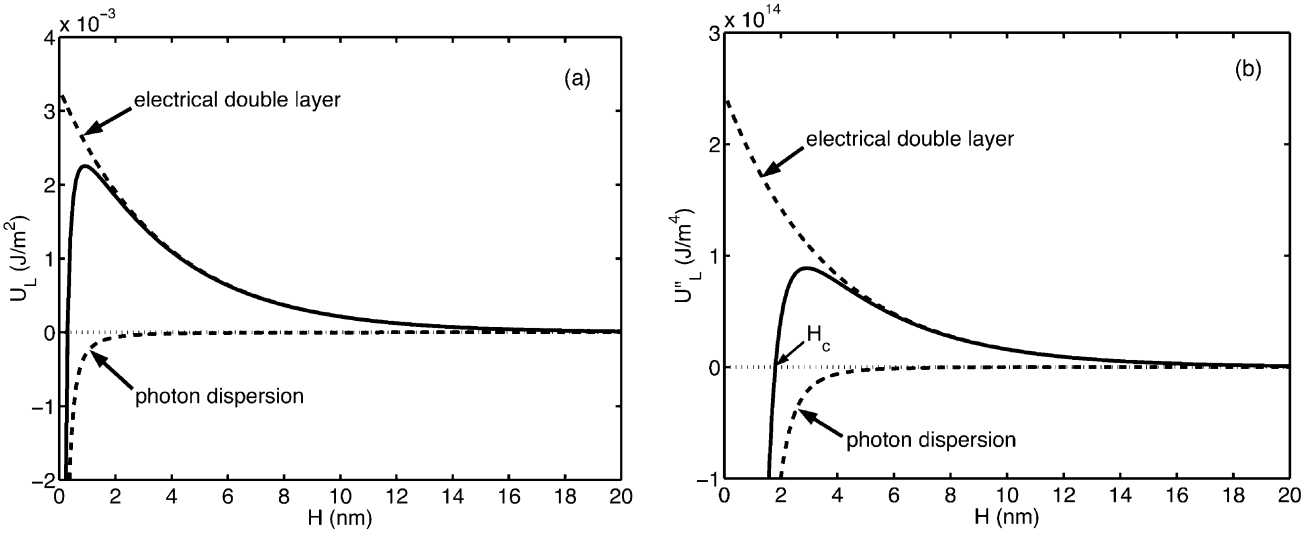

Fig. 4. (a) Combined interaction energy resulting from photon dispersion and electrical double layers as a function of separation; (b) Curvature of the interaction energy as a function of separation.

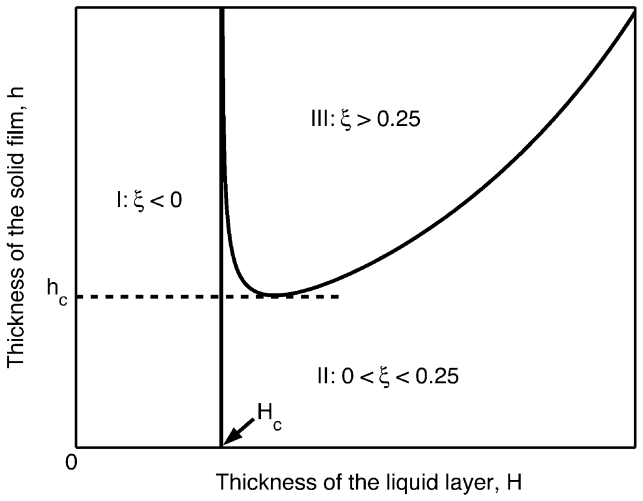

Fig. 6. A schematic h–H diagram of stability, under the combined interaction of photon dispersion and electrical double layer.

Fig. 6 schematically shows the stable and unstable regions in the h–H diagram under the combined interaction of photon dispersion and electrical double layer. In region I, $\xi<0$, and the flat film is unstable. In region II, $0<\xi<0.25$, the flat film is stable if $N>0$, but unstable if $N<0$. In region III, $\xi>0.25$, the flat film is stable. The dashed line indicates the critical thickness of the solid film.

4.4. Electron confinement

Next we consider a metal film on a substrate. It is common that a native oxide lies on top of the metal. At an elevated temperature, the metal creeps, but the oxide remains to be solid. The native oxide is typically very thin, just a few nanometers, and is subject to an inplane residual stress due to the oxidation process. A recent model has highlighted forces of two origins in a metal film: quantum confinement and charge transfer [31,32]. Here we consider quantum confinement only. As an estimate of the interaction energy, Suo and Zhang [32] consider electrons confined in a metal film by infinite potentials on both side and give an asymptotic expression,

$$U_L(H)=\frac{C}{H}, \tag{24}$$

where $C=\dfrac{3\pi^2\hbar^2 n}{32m}$, h is the Planck constant, m the electron mass, and n the number of free electrons per unit volume. For finite confinement potentials, the interaction energy has the same form as Eq. (24), but with a different constant C.

Substituting Eq. (24) into Eq. (12), we obtain that,

$$\xi=\frac{Eh^3C}{6(1-\nu^2)\left(\sigma h+\bar{f}\right)^2H^3}. \tag{25}$$

Because $\xi>0$, when the resultant membrane force in the oxide layer is tensile, the flat film is stable against perturbations of all wavenumbers. When the resultant membrane force is compressive, there exists a critical thickness H_c. When $H<H_c$, $\xi>0.25$ and the flat film is stable. When $H>H_c$, $0<\xi<0.25$ and the flat film is unstable. Using representative values, $n=5\times10^{28}$ m^{-3}, $E=100$ GPa, $\sigma=-100$ MPa, $h=10$ nm, $\bar{f}=0$, and $\nu=0.3$, we have $H_c\approx35$ nm.

5. Conclusions

A linear perturbation analysis has been performed to study the stability of very thin solid-on-liquid (SOL) structures. Flexural rigidity of the solid film stabilizes the flat film against perturbations of short wavelengths. Depending on its sign, the resultant membrane force, combining the surface stress and the residual stress in the solid film, can either stabilize or destabilize the film with perturbations of intermediate wavelengths. Depending on the shape of the interaction energy, concave up or down, the interfacial forces can either stabilize or destabilize the film with perturbations of long wavelengths. The importance of the surface stress depends on its contribution to the resultant membrane force compared to the residual stress. The relative importance of the flexural rigidity, the resultant membrane force, and the interfacial force is quantified by a dimensionless parameter ξ. Regardless of the physical origins of the interfacial forces, the stability analysis predicts that suitable interfacial forces may stabilize a solid film under compression or destabilize a film under tension. Specifically, the interfacial forces resulting from photon dispersion, electrical double layer, and electron confinement are considered, and their effects on SOL structures are estimated.

Acknowledgments

This work is supported by the National Science Foundation through grants CMS-9820713 and CMS-9988788, and by the Department of Energy through contract DE-FG02-99ER45787.

References

[1] Z. Suo, Int. J. Solids Struct. 37 (2000) 367.
[2] J.W. Verwey, J.Th.G. Overbeek, Theory of the Stability of Lyophobic Colloids, Elsevier, Amsterdam, Netherlands, 1948. Reprinted in 1999 by Dover Publications, New York.

[3] T. Sato, R. Ruch, Stabilization of Colloidal Dispersions by Polymer Adsorption, Marcel Dekker, Inc, New York and Basel, 1980.
[4] W.B. Russel, D.A. Saville, W.R. Schowalter, Colloidal dispersions, Cambridge University Press, Cambridge, England, 1989.
[5] O.L. Alerhand, D. Vanderbilt, R.D. Meade, J.D. Joannopoulos, Phys. Rev. Lett. 61 (1988) 1973.
[6] Z. Suo, W. Lu, J. Nanoparticle Res. 2 (2000) 333.
[7] K.D. Hobart, F.J. Kub, M. Fatemi, M.E. Twigg, P.E. Thompson, T.S. Kuan, C.K. Inoki, J. Electron. Mater. 29 (2000) 897.
[8] H. Yin, R. Huang, K.D. Hobart, Z. Suo, T.S. Kuan, C.K. Inoki, S.R. Shieh, T.S. Duffy, F.J. Kub, J.C. Sturm, J. Appl. Phys. 91 (2002) 9716.
[9] M.B. Williams, S.H. Davis, J. Colloid Interface Sci. 90 (1982) 220.
[10] S. Herminghaus, K. Jacobs, K. Mecke, J. Bischof, A. Fery, M. Ibnelhaj, S. Schlagowski, Science 282 (1998) 916.
[11] T.P. Witelski, A.J. Bernoff, Physica Part D 147 (2000) 155.
[12] M. Bestehorn, K. Neuffer, Phys. Rev. Lett. 87 (2001) art. no. 046101.
[13] J.W. Gibbs, Trans. Conn. Acad. III (1878) 343. Reprinted in 1993, The Scientific Papers of J. Willard Gibbs, vol.1, 314–315, by Ox Bow Press, Woodbridge, Connecticut.
[14] J.W. Cahn, Acta Metall. 28 (1980) 1333.
[15] J.R. Rice, T.J. Chuang, J. Am. Ceram. Soc. 64 (1981) 46.
[16] F. Spaepen, J. Mech. Phys. Solids 44 (1996) 675.
[17] C.H. Wu, J. Mech. Phys. Solids 44 (1996) 2059.
[18] L.B. Freund, J. Mech. Phys. Solids 46 (1998) 1835.
[19] R.C. Cammarata, Prog. Surf. Sci. 46 (1994) 1.
[20] R.C. Cammarata, K. Sieradzki, Annu. Rev. Mater. Sci. 24 (1994) 215.
[21] H. Ibach, Surf. Sci. Rep. 29 (1997) 193.
[22] N. Sridhar, D.J. Srolovitz, Z. Suo, Appl. Phys. Lett. 78 (2001) 2482.
[23] N. Sridhar, D.J. Srolovitz, B.N. Cox, Acta Materialia 50 (2002) 2547.
[24] R. Huang, Z. Suo, J. Appl. Phys. 91 (2002) 1135.
[25] R. Huang, Z. Suo, Int. J. Solids Struct. 39 (2002) 1791.
[26] S. Timoshenko, S. Woinowsky-Krieger, Theory of Plates and Shells, 2nd ed, McGraw-Hill, Inc, New York, 1987.
[27] J. Mahanty, B.W. Ninham, Dispersion Forces, Academic Press, New York, 1976.
[28] J. Israelachvili, Intermolecular and Surface Forces, 2nd ed, Academic Press, New York, 1992.
[29] D.Y.C. Chan, R.M. Pashley, L.R. White, J. Colloid Interface Sci. 77 (1980) 283.
[30] R.G. Horn, J. Am. Ceram. Soc. 73 (1990) 1117.
[31] Z.Y. Zhang, Q. Niu, C.K. Shih, Phys. Rev. Lett. 80 (1998) 5381.
[32] Z. Suo, Z.Y. Zhang, Phys. Rev. Part B 58 (1998) 5116.